Cellular/Molecular

Kv4.3-Mediated A-Type K^+ Currents Underlie Rhythmic Activity in Hippocampal Interneurons

Mathieu L. Bourdeau,* France Morin,* Charles E. Laurent, Mounia Azzi, and Jean-Claude Lacaille
Département de Physiologie, Groupe de Recherche sur le Système Nerveux Central, Université de Montréal, Montréal, Québec, Canada H3C 3J7

Hippocampal-dependent learning and memory processes are associated with theta frequency rhythmic activity. Interneuron and pyramidal cell network interactions underlie this activity, but contributions of interneuron voltage-gated membrane conductances remain unclear. We show that interneurons at the CA1 lacunosum-moleculare (LM) and radiatum (RAD) junction (LM/RAD) display voltage-dependent subthreshold membrane potential oscillations (MPOs) generated by voltage-gated tetrodotoxin-sensitive Na^+ and 4-aminopyridine (4-AP)-sensitive K^+ currents. They also exhibit prominent 4-AP-sensitive A-type K^+ currents, with gating properties showing activation at subthreshold membrane potentials. We found that LM/RAD cells are part of specific interneuron subpopulations expressing the K^+ channel subunit Kv4.3 and their transfection with Kv4.3 small interfering RNA selectively impaired A-type K^+ currents and MPOs. Thus, our findings reveal a novel function of Kv4.3-mediated A-type K^+ currents in the generation of intrinsic MPOs in specific subpopulations of interneurons that may participate in hippocampal theta-related rhythmic activity.

Key words: **theta rhythm; CA1 hippocampus; inhibitory interneurons; slice cultures; membrane potential oscillations; K^+ channels**

Introduction

Theta frequency rhythmic electroencephalographic activity generated in the hippocampus has been implicated in explorative behavior, learning/memory processes, and REM sleep (Winson, 1978; Bland, 1986; Vinogradova, 1995; Buzsaki, 2002; Cantero et al., 2003). Hippocampal theta oscillations arise from network activity and are essential in controlling temporal integration and modification of synaptic inputs (Buzsaki, 2002). Extrinsic inputs (Petsche et al., 1962), intrinsic conductances of pyramidal cells (Nunez et al., 1987), and network interactions between inhibitory interneurons and pyramidal cells contribute to theta activity (Klausberger et al., 2003; Somogyi and Klausberger, 2005). Hippocampal and entorhinal theta rhythms *in vivo* are driven by the medial septum (Petsche et al., 1962; Mitchell et al., 1982), but theta-like activity can be generated in isolated hippocampus by cholinergic agonists (MacVicar and Tse, 1989; Fischer et al., 1999). Moreover, theta-frequency range intrinsic membrane potential oscillations (MPOs) occur in entorhinal cortical neurons (Klink and Alonso, 1993), hippocampal CA1 pyramidal cells (Leung and Yim, 1991), and certain inhibitory interneurons (Chapman and Lacaille, 1999a), and likely contribute to theta activity (Chapman and Lacaille, 1999b).

In hippocampal and entorhinal neurons, MPOs arise from an interaction of voltage-dependent Na^+ and K^+ currents activated at subthreshold membrane potentials (Alonso and Llinas, 1989; Leung and Yim, 1991; Klink and Alonso, 1993; Chapman and Lacaille, 1999a,b; Hu et al., 2002). These ionic mechanisms contrast with Ca^{2+} and Ca^{2+}-activated K^+ currents implicated in oscillatory activity in other CNS neurons (Jahnsen and Llinas, 1984; Alonso and Llinas, 1992). However, it remains unclear which specific voltage-gated K^+ currents generate MPOs. In hippocampal interneurons, MPOs are prevented by Ba^{2+} and 4-aminopyridine (4-AP) but not by tetraethylammonium (TEA) (Chapman and Lacaille, 1999a). This pharmacological profile suggests that transient A-type K^+ currents or dendrotoxin-sensitive K^+ currents (I_D) may be involved in MPO generation (Rudy, 1988; Hurst et al. 1995; Locke and Nerbonne, 1997; Coetzee et al. 1999; Shi et al. 2000). Activation of MPOs at subthreshold membrane potentials (Chapman and Lacaille, 1999a) is also consistent with a potentially important role of these currents (Coetzee et al., 1999; Lien et al., 2002). Interestingly, neuronal A-type K^+ currents are associated with functions such as regulating firing rate (Rudy, 1988), shaping spike waveform (Zhang and McBain, 1995b) and controlling signal propagation in dendrites (Hoffman et al., 1997), but have not been linked to generating rhythmic activity. Therefore, our aim was to explore the role of voltage-gated A-type K^+ currents in interneuron MPOs. Moreover, because members of the Kv4 family of voltage-gated K^+ channel α subunits (Birnbaum et al., 2004) underlie somatodendritic A-type K^+ currents in many neuronal types (Shibata et al., 2000; Kim et al., 2005; Yuan et al., 2005) and because hippocampal CA1 interneurons highly express the Kv4.3

Received July 26, 2006; revised Jan. 15, 2007; accepted Jan. 15, 2007.

This work was supported by Canadian Institutes of Health Research Grant MT-10848, Fonds de la recherche en santé du Québec (Groupe de Recherche sur le Système Nerveux Central), and the Canada Research Chair Program (J.-C.L.; Canada Research Chair in Cellular and Molecular Neurophysiology). Plasmid constructs were kindly provided by M. Bouvier, J. M. Nerbonne, and A. Shrier. The antibodies against somatostatin (#56) and cholecystokinin (#9303) were kindly provided by CURE/Digestive Diseases Research Center, RIA Core, and National Institutes of Health Grant DK41301. We thank Julie Pepin for excellent technical assistance.

*M.L.B. and F.M. contributed equally to this work.

Correspondence should be addressed to Dr. Jean-Claude Lacaille, Département de Physiologie, Université de Montréal, Cas Postal 6128 Succursale Centre-ville, Montréal, Québec, Canada H3C 3J7. E-mail: jean-claude.lacaille@umontreal.ca.

M. Azzi's present address: Neurochem Incorporated, 275 Armand-Frappier Boulevard, Laval, Québec, Canada H7V 4A7.

DOI:10.1523/JNEUROSCI.3208-06.2007

 0270-6474/07/271942-12$15.00/0

subtype (Serodio and Rudy, 1998; Rhodes et al., 2004), we examined the role of Kv4.3 in A-type K^+ currents and MPOs in interneurons. Our results uncover a crucial role of Kv4.3 in mediating A-type K^+ currents and generating subthreshold intrinsic rhythmic activity in specific interneuron subpopulations.

Materials and Methods

Hippocampal slice preparation and culture. All animal procedures conformed to the animal welfare guidelines at Université de Montréal. Sixteen- to 30-d-old male rats (Sprague Dawley; Charles River, St-Constant, Quebec, Canada) were deeply anesthetized with halothane (Halocarbon Laboratories, River Edge, NJ) and acute hippocampal slices (300 μm thick) were prepared as described previously (Chapman and Lacaille, 1999a).

Organotypic hippocampal slice cultures were prepared and maintained as described (Stoppini et al., 1991). In brief, Sprague Dawley rats [postnatal day 7 (P7)–P12] rats were anesthetized and decapitated. The brain was removed and dissected in HBSS- (Invitrogen, Eugene, OR) based medium. Four-hundred-micrometer-thick corticohippocampal slices were obtained with a McIlwain tissue chopper (Campden Instruments, Lafayette, IN). Three to four slices were placed on Millicell culture plate inserts (Millipore, Bedford, MA) and incubated for 3 d in OptiMem- (Invitrogen) based medium at 37°C in a humidified atmosphere of 5% CO_2 and 95% air. Inserts were then transferred to neurobasal-based medium (Invitrogen). Slices were used for experiments after 3–12 d in culture.

Electrophysiology. Cells were viewed with an upright microscope (Axioskop; Zeiss, Oberkochen, Germany) equipped with Hoffmann optics (Modulation Optics, Greenvale, NY), a long-range water immersion objective (40×), and an infrared video camera (model 6500; Cohu, San Diego, CA). In the CA1 region, interneurons located at the border of strata lacunosum-moleculare and radiatum (LM/RAD), or pyramidal cells from stratum pyramidale (PYR) were visually identified and selected for recordings. All recordings were made at room temperature (20–22°C) using an Axopatch 200B amplifier (Molecular Devices, Foster City, CA). Signals were filtered at 2 kHz (8-pole Bessel filter) and digitized at 10 kHz on a Pentium-based computer using pClamp 7.0 or 9.0 (Molecular Devices). Whole-cell current-clamp recordings were made in artificial CSF (ACSF) containing the following (in mM): 124 NaCl, 26 $NaHCO_3$, 2.5 KCl, 1.25 NaH_2PO_4, 2 $CaCl_2$, 2 $MgSO_4$, 10 glucose (305 mOsm). Extracellular solutions were saturated with 95% O_2-5% CO_2. Recording pipettes (1.0 mm OD, 2–5 MΩ; World Precision Instruments, Sarasota, FL) were filled with the following (in mM): 140 K-gluconate, 5 NaCl, 10 HEPES, 0.5 EGTA, 2 $MgCl_2$, 2 ATP-Tris, 0.4 GTP-Tris, and 0.1% biocytin or 0.05% Oregon green dextran (285 mOsm, pH 7.2–7.3). The liquid junction potential was 14 mV and corrected. For MPO recordings, steady current injection was used to hold membrane potential at a level which generated occasional spontaneous action potentials, in the presence of antagonists of non-NMDA (CNQX, 20 μM), NMDA (AP5, 50 μM), and $GABA_A$ (bicuculline, 25 μM) receptors. Channel blockers tetrodotoxin (TTX) (0.2 μM), 4-AP (5 mM), 4-ethylphenylamino-1,2-dimethyl-6-methylaminopyrimidinium chloride (ZD-7288) (10 μM), and 10,10-bis(4-pyridinylmethyl)-9(10*H*)-anthracenone dihydrochloride (XE-991) (10 μM) were bath applied. When 5 mM 4-AP was applied, the $GABA_B$ receptor antagonist CGP55845A (1 μM) was also added. MPOs were analyzed during segments of membrane potential recordings with spectral analysis (peak frequency and total power between 1.5 and 5 Hz) using pClamp software as described previously (Chapman and Lacaille, 1999a). In experiments with recordings from cells expressing fluorescent proteins in transfected cultured slices, the antioxidant Trolox (0.04 mM) was added to the ACSF.

Voltage-clamp recordings (outside-out patches and whole-cell configuration) were made in ACSF containing the following (in mM): 125 NaCl, 25 $NaHCO_3$, 2.5 KCl, 1.25 NaH_2PO_4, 2 $CaCl_2$, 2 $MgCl_2$, 23 glucose (310 mOsm). Patch pipettes (1.0–1.2 mm outer diameter, 2–5 MΩ) were filled with solution containing the following (in mM): 120 K-gluconate, 20 KCl, 10 HEPES, 5 EGTA, 1 $MgCl_2$, 5 glutathione, 2 ATP-Tris, 0.4 GTP-Tris and 0.1% biocytin or 0.05% Oregon green dextran (Invitrogen) (300 mOsm). After achieving the whole-cell configuration, leakage and capacitative currents were subtracted on-line using a P/4 procedure. Series resistance was in the range of 5–15 MΩ and compensated by 40–60% during whole-cell voltage-clamp recordings. The liquid junction potential of the solution was 13 mV and corrected. A-type K^+ currents were obtained in the presence of channel blockers by using voltage step protocols and isolated with digital subtractions (Zhang and McBain, 1995a; Lien et al., 2002). The gating properties of A-type K^+ currents in interneurons were characterized using outside-out patch recordings. To obtain the activation curve, we calculated the chord conductance (g) by dividing respective peak currents at different test potentials by the driving force, assuming ohmic behavior and a reversal potential of −101 mV (measured using reversal of tail currents, data not shown). The activation curve was fitted with a Boltzmann function of the form: $g/g_{max} = (1 + \exp(-(V - V_{1/2})/k))^{-1}$, where g/g_{max} is the conductance normalized to its maximal value, V is the membrane potential, $V_{1/2}$ is the membrane voltage at which the current amplitude is half-maximum, and k is the slope factor. The inactivation curve was also fitted with the following Boltzmann function: $I/I_{max} = (1 + \exp((V - V_{1/2})/k))^{-1}$, where I/I_{max} is the current normalized to its maximal value. All drugs were purchased from Sigma (St. Louis, MO), except for ZD7288 and XE991 from Tocris Bioscience (Ellisville, MO), as well as TTX from Alomone Labs (Jerusalem, Israel).

HEK293 cells. Human embryonic kidney 293 (HEK293) cells were grown in DMEM, supplemented with 10% fetal bovine serum, penicillin/streptomycin, and L-glutamine (Wisent, St-Bruno, Quebec, Canada) at 37°C in a humidified atmosphere of 5% CO_2 and 95% air. HEK293 cells were seeded on glass coverslips 1 d before transfection and placed in 35 mm culture dishes containing DMEM. Whole-cell voltage-clamp recordings were made using an extracellular solution containing the following (in mM): 150 NaCl, 5 KCl, 1 $CaCl_2$, 2 $MgCl_2$, 10 HEPES, 25 glucose (330 mOsm). Pipettes (outer diameter, 1.2 mm; 2–5 MΩ) were filled with the following (in mM): 140 KCl, 1 $MgCl_2$, 5 EGTA, 10 HEPES and 2 ATP (315 mOsm). The liquid junction potential was 12 mV and corrected.

Constructs, siRNAs, and transfections. $pcDNA_3$-GFP_{10} vector [green fluorescent protein (GFP)] was obtained from Dr. M. Bouvier (Université de Montréal, Montréal, Quebec, Canada), pEYFP-C1 [enhanced yellow fluorescent protein (EYFP)] was obtained from Clontech Laboratories (Mountain View, CA), pbkCMV-rKv4.3 (Kv4.3) was a gift from Dr. J. M. Nerbonne (University of Washington, St. Louis, MO), and pHA-CMV-Kv4.2 (Kv4.2) was provided by Dr. A. Shrier (McGill University, Montréal, Quebec, Canada). All small interfering RNA (siRNA) were purchased from Dharmacon (Lafayette, CO). Commercial siControl (siRNA-CTL) and cyanine3-tagged siGLO (Cy3-siRNA-CTL) were used as nontargeting control siRNAs. siRNA-Kv4.3 target sequences for rat were ACUAGUCGCUCCAGCCUUAUU (sense sequence) and 5′-PUAAGGCUGGAGCGACUAGUUU (antisense sequence). HEK293 cells were transfected using Fugene 6 (Roche, Basel, Switzerland), following the manufacturer's instructions. Cotransfections were completed using 1.8 μg Kv4.3 cDNA and 0.2 μg GFP cDNA. For siRNA experiments, 10 μl of a 20 μM stock solution was added to the transfection mixture. Cells were incubated at 37°C in 5% CO_2 for 48–72 h (without siRNA) or 48 h (siRNA experiments) before recordings. Biolistic transfections of neurons in organotypic slice cultures (between 4 and 6 d in culture) were made using a Helios gene gun (Bio-Rad, Hercules, CA) following manufacturer's instructions. Gold beads (1.6 μm) were coated with 50 μg EYFP cDNA alone or with 160 μl of 20 μM duplex siRNA. Successful adhesion of siRNAs onto gold beads was verified using Cy3-siRNA-CTL (data not shown). Transfected slices were returned to the incubator for 48 h before experiments. GFP- or EYFP-expressing cells were selected for recordings using an upright microscope equipped with an epifluorescence Fluoarc System and appropriate filters (Zeiss).

Immunocytochemistry. For immunocytochemical detection of Kv4.3-channel subunit in physiologically characterized LM/RAD interneurons, cells were labeled with Oregon green dextran during recordings and hippocampal slices were fixed in 4% paraformaldehyde in 0.1 M phosphate buffer (PB, 4°C, overnight). Slices were cryoprotected in 30% sucrose and recut (40 μm thick) on a freezing microtome (SM2000R; Leica,

Nussloch, Germany). Sections were treated with 0.3% H_2O_2 (30 min), put in 0.5% blocking agent (30 min, TSA kit; PerkinElmer, Woodbridge, Ontario, Canada), and incubated in rabbit anti-Kv4.3 (1:1000, overnight, RT; Millipore, Temecula, CA). The next day, sections were placed in biotinylated goat anti-rabbit IgGs (1:200, 1 h; Jackson ImmunoResearch, West Grove, PA) in the avidin-biotin complex (Elite ABC kit; 1:200, 30 min; Vector Laboratories, Burlingame, CA) and in the tyramide amplification solution (1:100, 5 min; Perkin-Elmer). Sections were then reincubated in ABC solution (30 min) and placed in Texas Red-conjugated streptavidin (1:200, 1 h; Jackson ImmunoResearch). Sections were rinsed thoroughly between incubations and mounted in Prolong Antifade kit (Invitrogen). A similar protocol was used for detection of Kv4.3 in transfected HEK293 cells.

For double immunofluorescence detection of Kv4.3 and calcium binding proteins or peptides, male rats (25–28 d old; $n = 2$) were deeply anesthetized with sodium pentobarbital and perfused with 4% paraformaldehyde in 0.1 M PB. Brains were postfixed for 5 h and cryoprotected in 30% sucrose. The next day, sections were cut (30 μm in thickness) and incubated in Kv4.3 (1:1000) and mouse antibodies for calbindin (CB) D-28k (1:200; Sigma), parvalbumin (PV) (1:500; Millipore), somatostatin (SOM) [1:200; CURE, University of California, Los Angeles (UCLA)], or cholecystokinin (CCK) (1:200; CURE, UCLA). The Kv4.3 antibody was revealed as described above, except for streptavidin conjugated to Alexa Fluor 488 (1:200; Invitrogen) used as the fluorophore, whereas mouse antibodies were revealed with goat anti-mouse IgGs conjugated to cyanine5 (1:200, 1 h; Jackson ImmunoResearch). Sections were mounted in the Prolong Antifade kit and observed with a Zeiss LSM 510 confocal microscope system (Axioskop; Coherent, Santa Clara, CA) and appropriate filters. Fluorescent images of HEK293 and neurons in acute or cultured hippocampal slices were obtained with an Eclipse E600 microscope (Nikon, Tokyo, Japan) equipped with a Retiga 1300 camera (Q-Imaging, Canada) and a fluorescent lamp (Hamamatsu, Hamamatsu City, Japan). All images were exported and processed in Adobe (San Jose, CA) Photoshop 7.0.

To verify the specificity of antibodies, controls were done by either omitting primary antibodies or by preabsorbing the primary antibody with its respective antigen (according to the manufacturer's specifications) and, in each case, no visible staining was detected. We also confirmed the specificity of the Kv4.3 antibody from Millipore by using a monoclonal antibody against Kv4.3 (clone K75/41; University of California Davis-National Institute of Neurological Disorders and Stroke-National Institute of Mental Health Neuromab Facility, Davis, CA). A similar distribution of Kv4.3 immunopositive interneurons was observed in the CA1 area (see also Kollo et al., 2006) and a similar proportion of Oregon green-labeled LM/RAD interneurons exhibiting MPOs were found to be immunopositive for Kv4.3 (data not shown).

Statistical analysis. Data are presented as means ± SEM. Statistical comparisons between experimental groups were made using unpaired or paired Student's *t* tests (two-tailed) as appropriate. Differences were considered significant when $p < 0.05$.

Results

MPOs in LM/RAD interneurons depend on Na^+ and K^+ currents

Using whole-cell current-clamp recordings from visually identified LM/RAD interneurons in rat hippocampal slices maintained at room temperature, MPOs appear as fluctuations in membrane potential occurring at a frequency near 2 Hz (Fig. 1). However, during recordings at more physiological temperature (32°C), MPO frequency has been shown to be in the theta range (6–8 Hz) (Chapman and Lacaille 1999a). MPOs are generated by intrinsic membrane conductances and are independent of glutamate and $GABA_A$ receptor-mediated synaptic transmission because the antagonists AP5, CNQX, and bicuculline did not prevent them (Fig. 1*A*,*B*,*D*). The total power of MPOs, measured by spectral analysis, was significantly reduced to 8.6 ± 1.2% of control ($n = 24$) by −10 mV membrane hyperpolarization, whereas the peak frequency was unchanged (Fig. 1*E*), indicating that the amplitude but not the frequency of MPOs is dependent on membrane potential. The interplay of voltage-dependent Na^+ and K^+ conductances in the production of MPOs (Chapman and Lacaille, 1999a) was confirmed by application of the Na^+ channel blocker TTX (0.2 μM), which abolished action potentials and inhibited the power of MPOs to 8.9 ± 2.3% of control ($n = 9$) (Fig. 1*E*). The peak frequency was also augmented but this was a minor effect. Also, application of the K^+ channel blocker, 4-aminopyridine (4-AP, 5 mM) diminished the power of MPOs to 30.0 ± 4.5% of control ($n = 12$) without affecting the peak frequency (Fig. 1*A*,*E*). The inhibition of MPOs by 4-AP was reversible (92.4 ± 21.3% of control; $n = 5$). These results demonstrate that voltage-gated K^+ currents sensitive to millimolar concentration of 4-AP are implicated in the production of MPOs in LM/RAD interneurons.

To determine whether the hyperpolarization-activated cationic current (I_h), which contributes to MPOs in cells of the entorhinal cortex (Klink and Alonso, 1993), is involved in MPOs in interneurons, we applied the specific I_h blocker ZD7288 (10 μM). ZD7288 had no significant effect on total power (78.4 ± 13.9% of control; $n = 5$) or peak frequency of MPOs in interneurons (Fig. 1*B*,*E*). In contrast, inward rectification observed in interneurons in response to hyperpolarizing current (Maccaferri and McBain, 1996) was abolished by ZD7288 (rectification ratio, 1.30 ± 0.09 in control vs 1.00 ± 0.04 in ZD7288; $n = 5$; $p < 0.05$) (Fig. 1*C*), confirming the block of I_h currents in interneurons displaying MPOs. Thus, I_h does not contribute to the generation of MPOs in LM/RAD interneurons. To examine whether the muscarine-sensitive K^+ current (I_M), which is important for subthreshold resonance in hippocampal pyramidal cells (Hu et al. 2002), is involved in interneuron MPOs, we used the specific I_M blocker XE991 (10 μM) (Hu et al. 2002). Application of XE991 had no significant effect on the power (124.7 ± 17.7% of control; $n = 5$) and peak frequency of MPOs (Fig. 1*D*,*E*), but caused a membrane depolarization in interneurons (V_m, −62.2 ± 0.8 mV to −59.3 ± 0.9 mV; $n = 5$) consistent with inhibition of I_M (Hu et al. 2002). These results suggest that I_M is not necessary for the generation of MPOs in LM/RAD interneurons.

Properties of A-type K^+ currents and expression of Kv4.3 in LM/RAD interneurons

Because A-type K^+ currents are transient voltage-gated currents activated at subthreshold membrane potentials and sensitive to 4-AP (Serodio et al., 1996; Lien et al., 2002), we hypothesized that these currents could be involved in MPOs in LM/RAD interneurons. Thus, we characterized the biophysical properties of A-type K^+ currents in outside-out patches from LM/RAD interneurons. In the presence of TTX (0.5 μM) and TEA (20 mM), K^+ currents were evoked by 200 ms test pulses from a hyperpolarized membrane potential and consisted of rapidly inactivating and noninactivating components (Fig. 2*A*). In contrast, K^+ currents that were evoked by similar test pulses from a depolarized membrane potential were composed of only a noninactivating "delayed" component (Fig. 2*A*). A-type K^+ currents were isolated by subtracting the noninactivating component from the mixed rapidly inactivating and noninactivating currents (Fig. 2*A*) (Zhang and McBain, 1995a, Song et al., 1998). The mean amplitude of A-type K^+ currents evoked by a test pulse to 57 mV was 712.2 ± 85.9 pA ($n = 17$). The 20–80% rise time of A-type K^+ currents was 0.7 ± 0.1 ms ($n = 10$) whereas the inactivation phase (decay) was fitted by a biexponential function with time constants of τ_{fast} = 6.0 ± 0.3 ms and τ_{slow} = 22.8 ± 1.2 ms ($n = 9$; relative

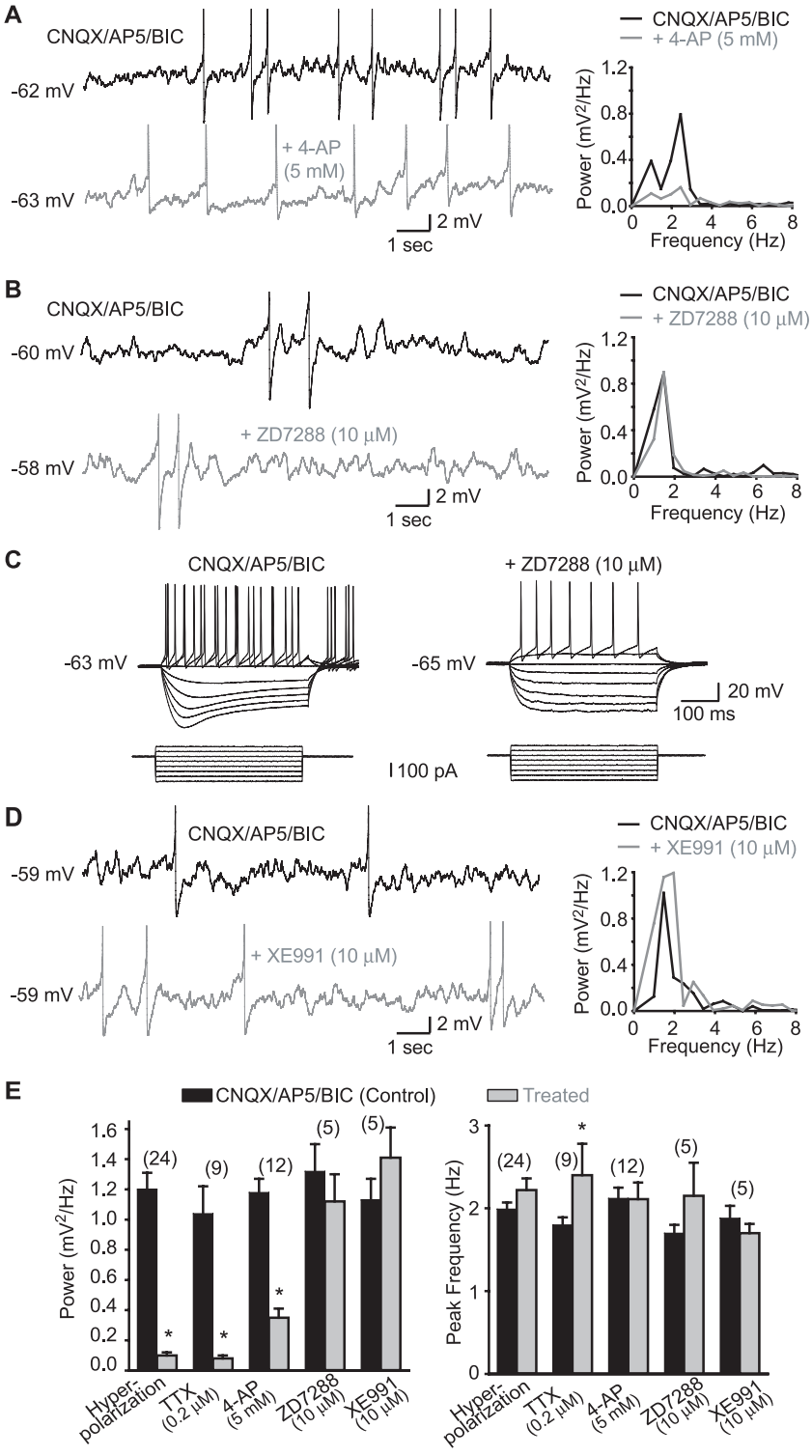

Figure 1. MPOs in LM/RAD interneurons in acute slices are dependent on 4-AP-sensitive K^+ currents but not on I_h or I_M. ***A***, MPOs from a representative interneuron (left) recorded at membrane potential near spike threshold in the presence of non-NMDA, NMDA, and $GABA_A$ receptor antagonists [CNQX, 20 μM; AP5, 50 μM; bicuculline (BIC), 25 μM; top trace]. In the same cell, MPOs are significantly reduced by application of 4-AP (5 mM; bottom trace). In this and other figures with traces showing MPOs, action potentials are truncated. Power spectra (right) of records from the same cell show the reduction of the power of MPOs by 4-AP. ***B***, Similar data from another cell showing that MPOs recorded near spike threshold are not diminished by ZD7288, a blocker of the h current (I_h). ***C***, Positive control experiments from the same cell as in ***B*** showing that the sag in the membrane response elicited by hyperpolarizing current injections and produced by I_h (control in CNQX/AP5/BIC; left) was blocked by ZD7288 (10 μM; right). ***D***, Representative traces from another interneuron showing that MPOs and corresponding power spectra are not reduced by XE991 (10 μM), a selective blocker of muscarine-sensitive K^+ current (I_M). ***E***, Summary bar graphs showing that the power of MPOs was significantly reduced by membrane hyperpolarization (V_m threshold −10 mV), TTX (0.2 μM), and 4-AP (5 mM) but not by ZD7288 (10 μM) or XE991 (10 μM), whereas the peak frequency of MPOs was generally unchanged. *$p < 0.05$.

amplitude contributions τ_{fast} = 65.0 ± 6.9% and τ_{slow} = 35.0 ± 7.0%). Additionally, the time course of recovery from inactivation for A-type K^+ currents (measured by test pulses to 57 mV from holding of −73 mV) was quite rapid (40.4 ± 1.5 ms; $n = 6$). The activation curve was fitted by a Boltzmann function with half-maximal ($V_{1/2}$) activation at −16.9 ± 0.2 mV and a slope factor (k) of 15.8 ± 0.9 mV ($n = 14$) (Fig. 2*C*). The inactivation of A-type K^+ currents was studied by applying 1 s prepulses followed by a test pulse (Fig. 2*B*). The inactivation curve was also described by a Boltzmann function with a midpoint potential ($V_{1/2}$) of −86.1 ± 0.1 mV and a slope factor (k) of 12.1 ± 0.4 mV ($n = 10$) (Fig. 2*C*). The intersection of the activation and inactivation curves for A-type K^+ currents (Fig. 2*C*) indicated the presence of a window current near subthreshold membrane potentials at which MPOs were observed. Thus, our results indicate that LM/RAD interneurons display prominent A-type K^+ currents with gating properties consistent with activation at subthreshold membrane potentials. Because MPOs are sensitive to 4-AP, we examined the effects of 4-AP on A-type K^+ currents in outside-out patches (Fig. 2*A*). The peak amplitude of A-type K^+ currents was significantly reduced by 5 mM 4-AP (61.7 ± 9.9% of control; $n = 8$; $p < 0.05$) without significant effects on decay time constants (τ_{fast}, 80.8 ± 17.6% of control; τ_{slow}, 85.7 ± 34.9% of control; $n = 6$). The effects of 4-AP were partially reversible and the amplitude of A-type K^+ currents returned to 79.4 ± 8.3% of control ($n = 4$) after wash-out. Application of a lower concentration of 4-AP (60 μM) did not significantly affect the amplitude of A-type K^+ currents (94.6 ± 31.7% of control; $n = 3$) nor their decay time constants (τ_{fast}, 73.2.±20.9% of control; τ_{slow}, 89.8 ± 21.3% of control; $n = 3$). Thus, these results indicate that A-type K^+ currents, like MPOs, are sensitive to 4-AP.

Because K^+ channels composed of Kv4 subunits are major contributors of somatodendritic A-type K^+ currents (Serodio et al., 1996; Birnbaum et al., 2004) and because CA1 interneurons highly express Kv4.3 mRNA (Serodio and Rudy, 1998) and protein (Rhodes et al., 2004), we examined whether interneurons displaying A-type K^+ currents and MPOs also express Kv4.3 by combining cell labeling during whole-cell recording with immunohistochemistry. Ninety-three percent

of interneurons filled with Oregon green during whole-cell recordings that displayed A-type K^+ currents in outside-out patch recordings were also immunopositive for Kv4.3 ($n = 14$) (Fig. 2*D*). The Kv4.3 protein was located in the somatodendritic compartment of interneurons. Moreover, 71% percent of Oregon green-filled interneurons that showed MPOs were also Kv4.3-immunopositive ($n = 24$) (Fig. 2*E*). These results demonstrate that Kv4.3 is present in the somatodendritic compartment of LM/RAD interneurons displaying A-type K^+ currents and MPOs, consistent with a possible implication of this K^+ channel subunit in these physiological responses.

Kv4.3-mediated A-type K^+ currents and functional knockdown in recombinant system

With the goal of interfering with Kv4.3 expression in interneurons, we first established that siRNA could be used for functional knockdown of Kv4.3-mediated A-type K^+ currents in a heterologous expression system. HEK293 cells were cotransfected with Kv4.3 cDNA and GFP constructs. Immunocytochemistry was used first to establish that GFP-positive cells were immunopositive for Kv4.3 (Fig. 3*A*) ($n = 4$ cultures, 2 experiments). Then, whole-cell recordings were obtained from GFP-positive HEK293 cells. K^+ currents were evoked by test pulses from a hyperpolarized membrane potential and consisted of transient and sustained components (Fig. 3*B*). K^+ currents evoked from a depolarized membrane potential consisted of only sustained K^+ currents. Peak A-type K^+ currents, isolated using digital subtraction and elicited by voltage step to 28 mV, had a current density ($I_{density}$) of 79.7 ± 14.0 pA/pF ($n = 30$) (Fig. 3*B*). Cells transfected with GFP alone lacked such transient A-type K^+ currents ($I_{density}$, 5.6 ± 1.6 pA/pF) and only presented endogenous sustained K^+ currents (Fig. 3*B*) (Yu and Kerchner, 1998). Therefore, expression of Kv4.3 in HEK293 cells results in A-type K^+ currents (Barry et al., 1998; Cotella et al., 2005). Next, we ascertained the efficacy of a siRNA sequence targeting Kv4.3 mRNA (siRNA-Kv4.3) in preventing the expression of Kv4.3-mediated A-type K^+ currents. Efficient delivery of siRNAs to HEK293 cells was assessed using a cyanine3-tagged nontargeting siRNA (Cy3-siRNA-CTL) (Fig. 3*C*) ($n = 5$ cultures, 2 experiments). Using electrophysiological recordings, we observed that cotransfection of Kv4.3, GFP, and siRNA-Kv4.3 significantly reduced Kv4.3-mediated A-type K^+ currents ($I_{density}$, 36.7 ± 12.0% of control; $n = 20$) compared with cells cotransfected with Kv4.3, GFP, and a non targeting siRNA sequence (siRNA-CTL; $n = 19$) (Fig. 3*D*). In contrast, the endogenous sustained K^+ currents were unaffected by siRNA-Kv4.3 transfection ($I_{density}$, 76.9 ± 8.6% of control; $n = 20$) (Fig. 3*D*). To verify the specificity of Kv4.3 siRNA, we expressed the closely related Kv4.2 subunit in HEK293 cells. When Kv4.2, GFP, and siRNA-CTL were cotransfected in HEK293 cells, typical transient A-type K^+ currents were observed ($I_{density}$, at 28 mV, 67.9 ± 19.1 pA/pF;

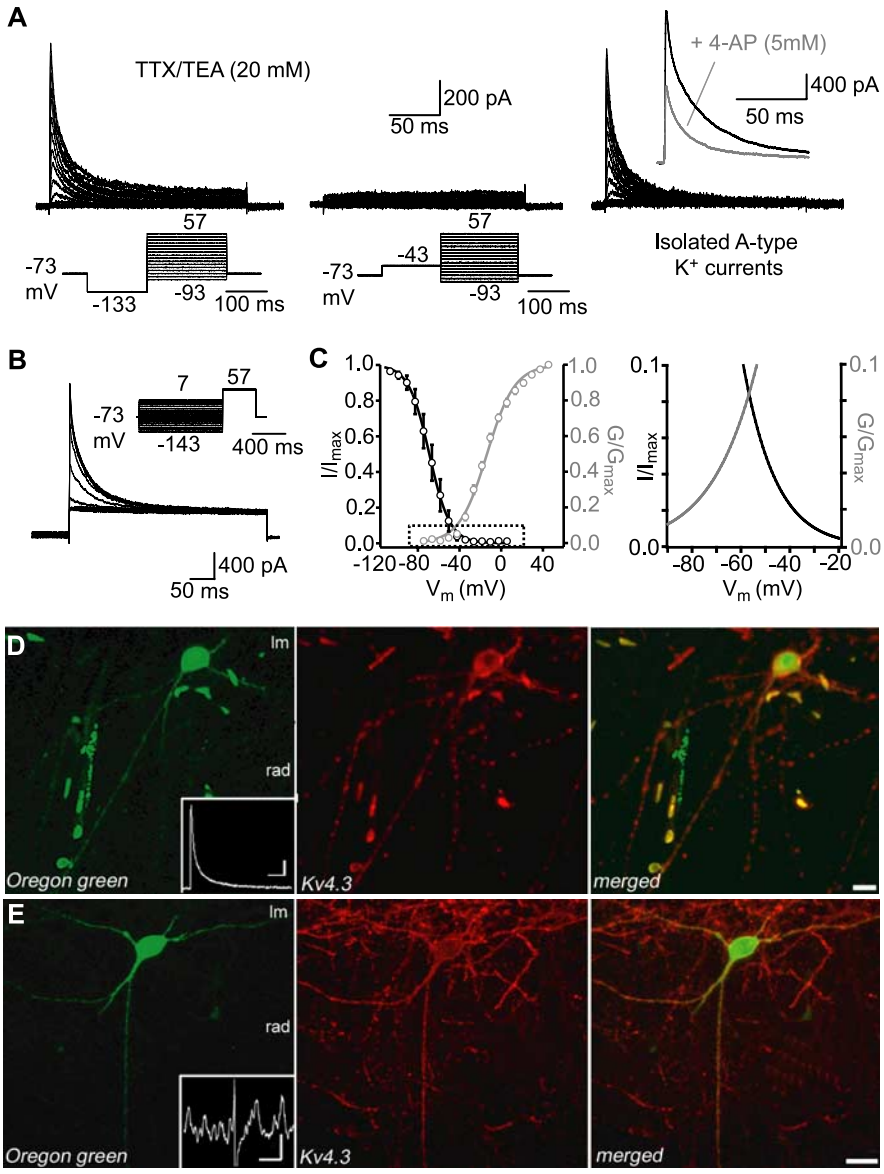

Figure 2. Properties of A-type K^+ currents and expression of Kv4.3 in LM/RAD interneurons in acute slices. ***A***, K^+ currents were recorded from outside-out patches pulled from somata of interneurons in the presence of TTX (0.5 μM) and TEA (20 mM). K^+ currents composed of rapidly inactivating and noninactivating components were evoked by test pulses to potentials between −93 and 57 mV (200 ms) from a potential of −133 mV (150 ms) (left), whereas currents composed of only a noninactivating component were evoked from a potential of −43 mV (middle). Digital subtraction resulted in the isolation of A-type K^+ currents (right) and inset shows reduction of A-type K^+ currents from another interneuron (elicited by a test pulses to 57 mV) by 5 mM 4-AP. ***B***, Inactivation of A-type K^+ currents was studied by applying 1 s prepulses between −143 and 7 mV followed by a pulse to 57 mV (400 ms). ***C***, Mean activation ($n = 14$) and inactivation ($n = 10$) curves of A-type K^+ currents were fitted using a Boltzmann function (left). Boxed area is shown enlarged at the right, illustrating the intersection of activation and inactivation curves and window current near threshold. ***D***, Confocal image of an Oregon green-filled interneuron (left) from which A-type K^+ currents were recorded in outside-out patch (inset; calibration: 200 pA, 25 ms). Confocal image shows immunolabeling for Kv4.3 in the same section (middle) and indicates that the protein is found in the soma and dendritic comportments. Merged images (right) show colocalization. ***E***, Example of a different Oregon green-labeled interneuron (left), which displayed MPOs during whole-cell recordings (inset; calibration: 2 mV, 1 s). This interneuron was also immunopositive for Kv4.3 (middle and right images). Scale bars: ***D***, 20 μm; ***E***, 10 μm.

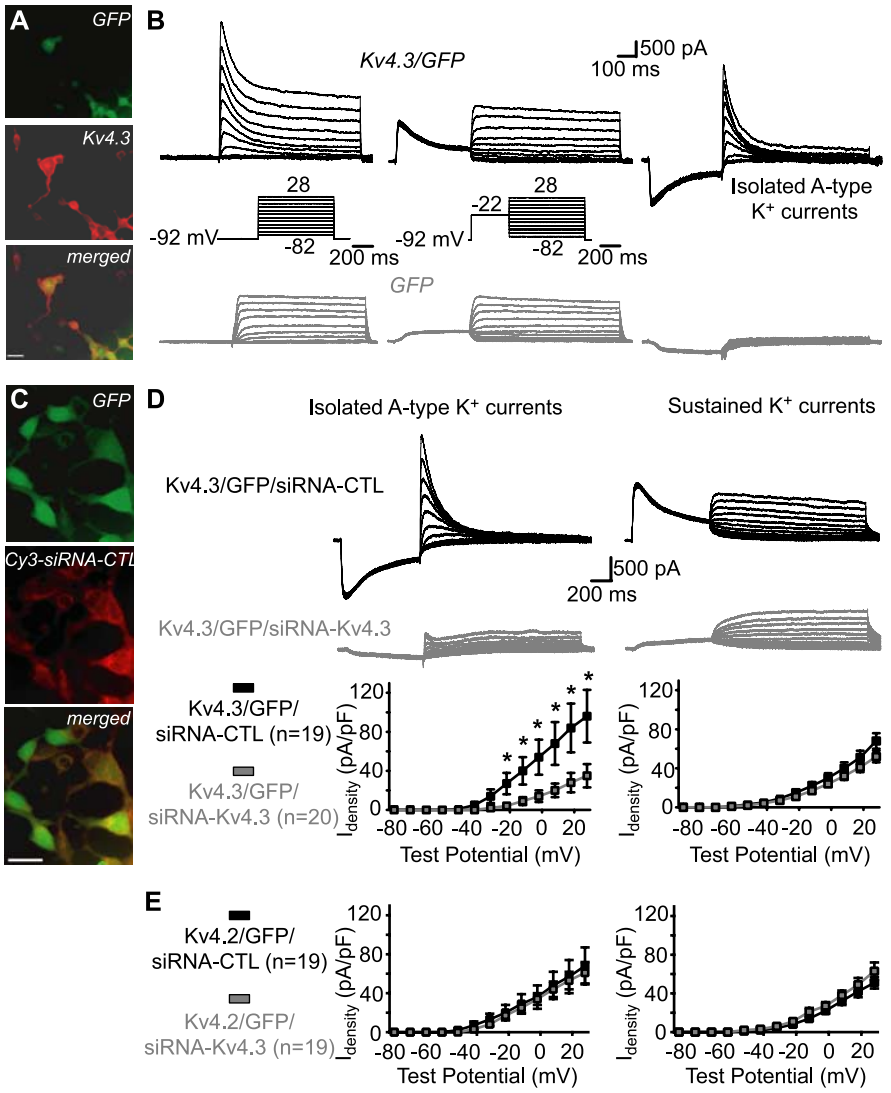

Figure 3. Kv4.3-mediated A-type K^+ currents and functional knockdown by siRNA in HEK293 cells. ***A***, Fluorescence images showing that GFP-expressing cells cotransfected with Kv4.3 (top) were immunopositive for Kv4.3 (middle and bottom). Scale bar, 25 μm. ***B***, In cells cotransfected with Kv4.3 and GFP (top traces), prominent A-type K^+ currents were isolated (right) by subtracting the sustained K^+ currents elicited by voltage jumps from a depolarized potential (middle) from the total K^+ currents evoked by voltage steps from a hyperpolarized potential (left). A-type K^+ currents were absent in cells transfected with GFP only (bottom traces). ***C***, Fluorescence images showing that GFP-expressing cells (top) cotransfected with Kv4.3 and a cyanine3-tagged nontargeting control siRNA (Cy3-siRNA-CTL) colocalized the fluorescently tagged siRNA (middle and bottom). Scale bar, 25 μm. ***D***, Traces from representative cells (top and middle) and summary graphs for all cells (bottom; $*p < 0.05$) illustrating that cotransfection of Kv4.3, GFP, and a nontargeting control (siRNA-CTL) resulted in large A-type K^+ currents, whereas cotransfection of Kv4.3, GFP, and siRNA targeting Kv4.3 (siRNA-Kv4.3) prevented expression of A-type K^+ currents (left). In contrast, endogenous sustained K^+ currents were not different in the same cells (right), indicating a selective functional knockdown of A-type currents. ***E***, Summary graphs for all cells from control experiments with transfection of Kv4.2, showing that Kv4.2-mediated A-type K^+ currents were similar in cells cotransfected with siRNA-CTL or siRNA-Kv4.3 (left). Sustained K^+ currents were also similar in both groups (right), indicating a selective functional knockdown of Kv4.3-mediated A-type K^+ currents.

$n = 19$) (Fig. 3*E*). After cotransfection of Kv4.2, GFP, and siRNA-Kv4.3, Kv4.2-mediated A-type K^+ currents were not different from control ($I_{density}$, 89.7 ± 16.4% of control; $n = 19$) (Fig. 3*E*). Hence, our results indicate a selective functional knockdown of Kv4.3-mediated A-type K^+ currents in recombinant system by Kv4.3 siRNA (Cotella et al., 2005).

Kv4.3 siRNA selectively reduces A-type K^+ currents in LM/RAD interneurons

To evaluate the contribution of Kv4.3 to A-type K^+ currents in interneurons, we used biolistic transfection of Kv4.3 siRNA in slice cultures (Govek et al., 2004). First, we established that whole-cell K^+ currents were similar in LM/RAD interneurons in cultured compared with acutely isolated slices. In TTX (1 μM), cadmium chloride ($CdCl_2$, 150 μM), and TEA (1 mM), whole-cell K^+ currents were composed also of transient and noninactivating components (Fig. 4*A*). Moreover, A-type K^+ currents had a similar $I_{density}$ and sensitivity to 4-AP in interneurons in cultured and acute slices (supplemental Table 1, available at www.jneurosci.org as supplemental material). A-type K^+ currents were also comparable in interneurons biolistically transfected with EYFP in comparison to untransfected (Fig. 4*B*, supplemental Table 1, available at www.jneurosci.org as supplemental material). Finally, using biocytin labeling, we verified that EYFP-expressing interneurons were nonpyramidal cells (Fig. 4*B*,*C*) with morphological characteristics similar to those of LM/RAD cells in acute hippocampal slices (Chapman and Lacaille, 1999a). Thus, EYFP-expressing LM/RAD interneurons in slice cultures exhibit A-type K^+ currents and cellular properties similar to interneurons in acute slices.

Next, we assessed the functional consequence of Kv4.3 siRNA transfection on A-type K^+ currents in LM/RAD interneurons. We verified that basic membrane properties and A-type K^+ currents of interneurons transfected with EYFP and siRNA-CTL were similar (supplemental Table 1, available at www.jneurosci.org as supplemental material). In contrast, in interneurons cotransfected with EYFP and Kv4.3 siRNA, the peak $I_{density}$ of A-type K^+ currents was significantly reduced (38.1 ± 8.0% of control; $n = 6$; $p < 0.05$) (Fig. 4*D*) compared with interneurons cotransfected with EYFP and control siRNA. Kv4.3 siRNA transfection did not affect activation ($V_{1/2} = -3.0 \pm 2.0$ mV, $k = 13.4 \pm 1.3$ mV, $n = 7$ for control siRNA; $V_{1/2} = 0.3 \pm 2.4$ mV, $k = 10.4 \pm 0.3$, $n = 6$ for Kv4.3 siRNA) or inactivation ($V_{1/2} = -61.5 \pm 3.3$ mV, $k = -9.0 \pm 0.9$ mV, $n = 5$ for control siRNA; $V_{1/2} = -58.1 \pm 5.2$ mV, $k = -9.5 \pm 0.7$, $n = 4$ for Kv4.3 siRNA) properties of A-type K^+ currents. Moreover, delayed rectifier K^+ currents were not significantly affected by Kv4.3 siRNA transfection ($I_{density}$, 131.5 ± 31.0% of control; $n = 6$) (Fig. 4*D*). Thus, the functional knockdown produced by siRNA-Kv4.3 is selective to A-type K^+ currents. We further established the selectivity of the functional knockdown produced by Kv4.3 siRNA by recordings of A-type K^+ currents in CA1 pyramidal cells, which are thought to be mostly mediated by Kv4.2 rather than Kv4.3 (Serodio and Rudy, 1998; Rhodes et al., 2004; Kim et al., 2005). Again, A-type K^+ currents were similar in EYFP-transfected and untransfected pyramidal cells (89.5 ± 17.5% of control; $n = 5$)

(Fig. 5*A–C*). Moreover, transfection with Kv4.3 siRNA did not alter either A-type (100.7 ± 30.9% of control; $n = 5$) or delayed rectifier (89.8 ± 14.7% of control; $n = 5$) K^+ currents in pyramidal cells compared with control siRNA transfection (Fig. 5*D*). Thus, Kv4.3 siRNA transfection selectively reduced A-type K^+ currents in interneurons, consistent with the cell-type specific expression of Kv4.3 in CA1 hippocampus.

Kv4.3 siRNA impairs MPOs in LM/RAD interneurons

Next, we examined the functional consequence of reducing A-type K^+ currents by Kv4.3 siRNA transfection on interneuron excitability and rhythmic activity. First, because Kv4-mediated A-type K^+ currents shape action potential waveform in pyramidal and Purkinje cells (Shibata et al., 2000; Kim et al., 2005; Yuan et al., 2005), we verified the effects of Kv4.3 siRNA transfection on interneuron action potential properties. Action potential amplitude (Fig. 6*B*), threshold and afterhyperpolarization (supplemental Table 1, available at www.jneurosci.org as supplemental material) were not significantly changed after Kv4.3 versus control siRNA transfection. In contrast, action potential duration at half amplitude ($APD_{half\text{-}width}$) was significantly longer in interneurons transfected with Kv4.3 versus control siRNA (154.0 ± 10.8% of control; $n = 10$; $p < 0.05$) (Fig. 6*A*,*B*). Again, as with other membrane properties tested, $APD_{half\text{-}width}$ was similar in EYFP-expressing and untransfected interneurons (supplemental Table 1, available at www.jneurosci.org as supplemental material). Application of 4-AP (5 mM), which blocks A-type K^+ currents, also significantly increased $APD_{half\text{-}width}$ (325.7 ± 60.8% of control; $p < 0.05$; $n = 5$) (Fig. 6*A*,*B*). 4-AP did not significantly change action potential amplitude (102.5 ± 2.2% of control), threshold (111.5 ± 4.6% of control), or AHP amplitude (101.8 ± 13.5% of control) in the same cells. Having verified that Kv4.3 siRNA affected action potential waveform in interneurons, we next determined the contribution of Kv4.3-mediated A-type K^+ currents to subthreshold MPOs in interneurons. MPOs were present in LM/RAD interneurons in cultured slices (Fig. 6) but their power was smaller and peak frequency elevated in comparison to acute slices (supplemental Table 1, available at www.jneurosci.org as supplemental material). Other MPO properties were generally similar to those in interneurons in acute slice: prevented by membrane hyperpolarization (8.3 ± 1.4% of control; $n = 22$), 0.2 μM TTX (7.7 ± 3.1% of control; $n = 6$), and 5 mM 4-AP (26.8 ± 8.1% of control; $n = 5$) (compare Figs. 1, 6*C*,*D*). However, transfection of Kv4.3 siRNA impaired MPOs in interneurons. The power of MPOs was significantly decreased in interneurons transfected with Kv4.3 siRNA compared with control siRNA (53.3 ± 12.5% of control; $p < 0.05$; $n = 10$), whereas the peak frequency of MPOs was unchanged (Fig. 6*E*,*F*). Overall, these data show that Kv4.3 siRNA, which produced a functional knockdown of A-type K^+ currents, resulted in inhibition of MPOs and broadening of action potentials. Thus, Kv4.3-mediated A-type K^+ currents play a critical role in subthreshold membrane potential oscillations, in addition to regulating action potential firing, in interneurons.

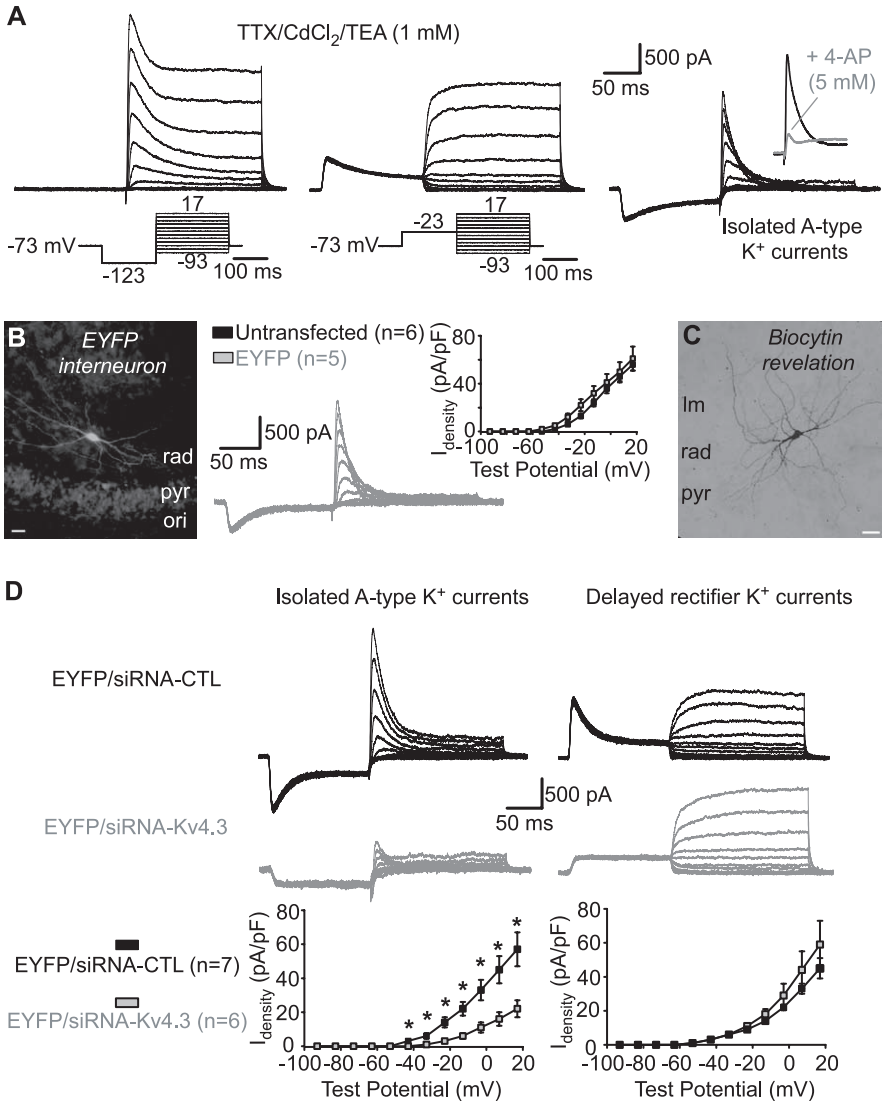

Figure 4. Kv4.3 siRNA reduces A-type K^+ currents in interneurons in slice cultures. ***A***, Whole-cell K^+ currents recorded from interneurons in TTX (1 μM), $CdCl_2$ (150 μM), and a low concentration of TEA (1 mM). Total K^+ currents activated by test pulses from a hyperpolarized potential consisted of rapidly inactivating and delayed components (left). Delayed rectifier K^+ currents evoked by test pulses from a depolarized potential (middle) were subtracted to isolate A-type K^+ currents (right). Inset shows sensitivity of A-type K^+ currents to 5 mM 4-AP. ***B***, Fluorescence image of an EYFP-expressing LM/RAD interneuron (left). Traces from a representative EYFP-expressing interneuron showing isolated A-type K^+ currents are shown in the middle. A summary graph illustrating similar A-type K^+ current density in untransfected and EYFP-expressing interneurons is shown at the right. ***C***, Example of biocytin labeling of an EYFP-expressing interneuron showing typical nonpyramidal morphology of LM/RAD interneurons. ***D***, Traces from representative interneurons (top) and summary graphs for all cells (bottom), indicating that transfection of Kv4.3 siRNA selectively reduced A-type K^+ current density (left) and did not affect delayed rectifier K^+ currents (right), compared with transfection with control siRNA. Scale bars: ***B***, ***C***, 25 μm. *$p < 0.05$.

Specific interneuron subpopulations expressing Kv4.3

We investigated next in more detail the CA1 interneuron subpopulations that express Kv4.3, using double immunofluores-

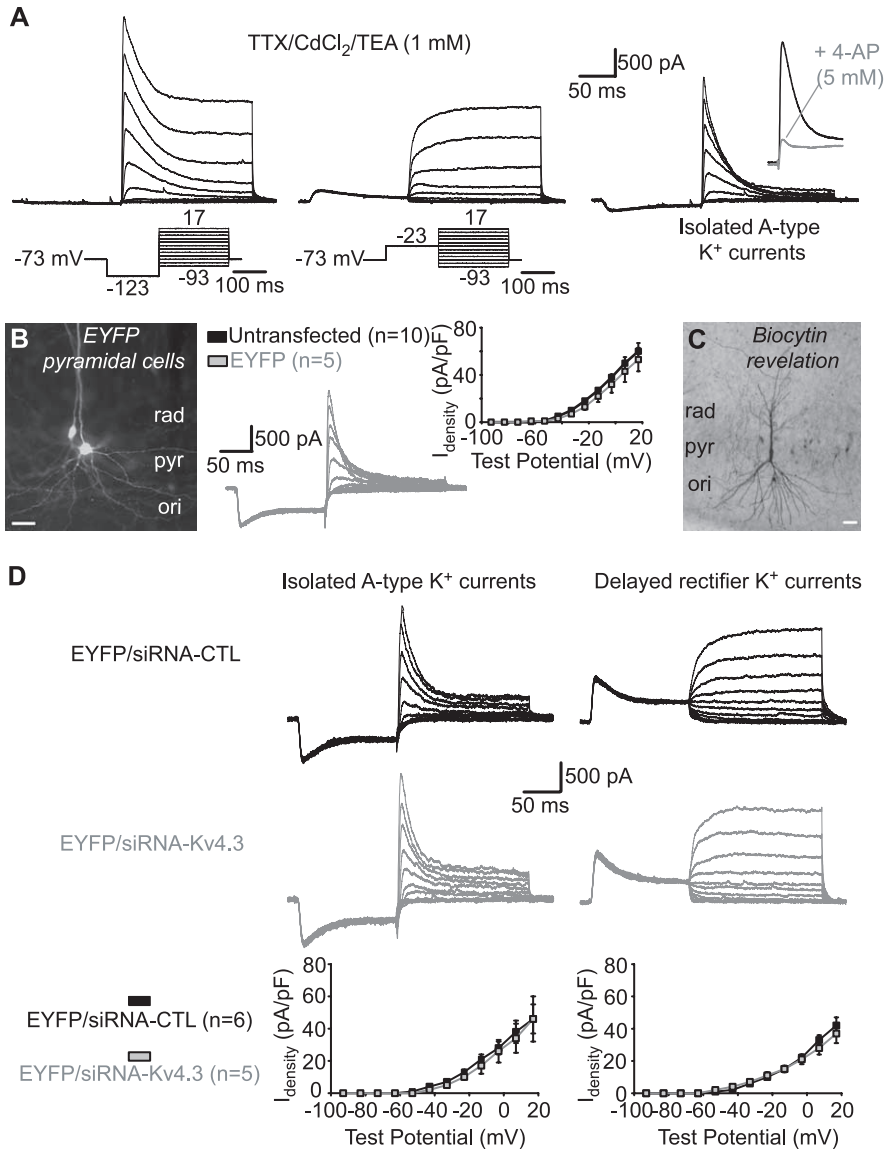

Figure 5. Kv4.3 siRNA did not affect A-type K^+ currents in CA1 pyramidal cells in slice cultures. ***A***, Total whole-cell K^+ currents (left) were composed of rapidly inactivating A-type (right) and delayed rectifier (middle) K^+ currents in pyramidal cells. A-type K^+ currents were inhibited by 4-AP (inset). ***B***, Fluorescence image of EYFP-expressing pyramidal cells (left). Traces from a representative EYFP-expressing pyramidal cell (middle) and summary graph for all cells (right) showing similar A-type K^+ current density in untransfected and EYFP-expressing pyramidal cells are shown. ***C***, Example of biocytin labeling of an EYFP-expressing pyramidal cell. ***D***, Traces from representative pyramidal cells (top) and summary graphs (bottom) illustrating that A-type (left) and delayed rectifier (right) K^+ current density were unchanged by Kv4.3 compared with control siRNA transfection. Scale bars: ***B***, ***C***, 25 μm.

cence against Kv4.3 and specific markers of interneuron subpopulations, the Ca^{2+}-binding proteins PV and CB, and the peptides SOM and CCK (Freund and Buzsaki, 1996). Interneurons immunopositive for each marker were first quantified according to their soma location within hippocampal CA1 layers [oriens/alveus (O/A), PYR, RAD, and LM] and then the proportion of interneurons in each layer, which colocalized Kv4.3 was assessed (Table 1). The majority of PV-immunopositive interneurons (81/84 neurons) were located within the pyramidal layer and only 12% of these cells coexpressed Kv4.3 (Fig. 7*A*). Calbindin-positive neurons were found in all hippocampal layers but Kv4.3 colocalization was higher in RAD and LM (50 and 70%, respectively) than O/A and PYR (20% each) (Fig. 7*B*). Somatostatin-positive neurons were mostly found in O/A, however very few of these SOM-positive cells colocalized Kv4.3 (13%) (Fig. 7*C*). Interestingly, the small proportion of SOM-positive cells found in PYR showed a high percentage of Kv4.3 colocalization (80%). Cholecystokinin-immunopositive neurons were distributed in all hippocampal layers but the majority was located in LM. The proportion of CCK-positive interneurons coexpressing Kv4.3 was highest in LM (88%), less in PYR and RAD (25 and 33%, respectively), and null in O/A (Fig. 7*D*). Therefore, some interneuron subpopulations preferentially express Kv4.3 and include CCK-positive interneurons in LM, CB-positive interneurons in RAD and LM, and SOM-positive interneurons of PYR. Thus, Kv4.3 may play a critical role in A-type K^+ currents and rhythmic activity in these specific CA1 interneuron subpopulations.

Discussion

Our principal findings are that hippocampal interneurons display subthreshold MPOs generated by an interplay of Na^+ and 4-AP-sensitive A-type K^+ currents, independent of hyperpolarization-activated cationic currents I_h, and muscarine-sensitive K^+ currents, I_M. We show that A-type K^+ currents are prominent in LM/RAD interneurons, have a window of activation at subthreshold membrane potentials, and are inhibited by 4-AP. Kv4.3 α-subunits of K^+ channels mediate LM/RAD interneuron A-type K^+ currents because (1) interneurons with A-type K^+ currents and MPOs were immunopositive for Kv4.3, (2) Kv4.3 expression generated A-type K^+ currents in HEK293 cells, and (3) Kv4.3 siRNA transfection functionally knocked-down A-type K^+ currents in HEK293 cells and LM/RAD interneurons. Kv4.3 siRNA-induced impairment was K^+ current- and cell type-selective as Kv4.2-mediated A-type K^+ currents were unchanged in HEK293 cells, sustained/delayed rectifier K^+ currents unaffected in HEK293 cells or interneurons, and A-type currents unimpaired in CA1 pyramidal cells. Kv4.3 siRNA transfection prevented interneuron MPOs and broadened action potentials, uncovering a critical role of Kv4.3 A-type K^+ currents in MPO generation. Finally, specific interneuron subpopulations preferentially expressed Kv4.3: cholecystokinin-positive interneurons of LM, calbindin-positive interneurons of RAD and LM, and somatostatin-positive interneurons of PYR. Our findings reveal a novel role for Kv4.3-mediated A-type K^+ currents in the generation of intrinsic MPOs in specific subpopulations of interneurons, which are important for CA1 hippocampal rhythmic activity.

Our findings provide novel evidence about intrinsic membrane currents critically underlying LM/RAD interneuron

MPOs. Consistent with results in CA1 pyramidal cells (Leung and Yim, 1991) and entorhinal stellate cells (Klink and Alonso, 1993), TTX-sensitive Na^+ currents are key contributors to MPO generation in LM/RAD interneurons (Chapman and Lacaille, 1999a). Because MPOs are present at subthreshold membrane potentials in absence of sustained repetitive spiking, persistent subthreshold Na^+ currents are implicated in interneurons, as in entorhinal cells (Klink and Alonso, 1993). However, other membrane currents involved in rhythmic activity contribute in a cell type-specific manner. First, nonselective cationic currents I_h, critical for MPOs in entorhinal stellate cells (Klink and Alonso, 1993; Dickson et al., 2000) and for subthreshold theta-frequency resonance in CA1 pyramidal cells (Hu et al., 2002), are not implicated in interneurons because interneuron MPOs were not prevented by the selective I_h blocker ZD7288, or by extracellular Cs^+ (Chapman and Lacaille, 1999a). Second, muscarine-sensitive K^+ currents I_M, important for CA1 pyramidal cell theta-frequency resonance (Hu et al., 2002), appear not to be involved because MPOs are unaffected by the selective I_M blocker, XE991. Finally, Ca^{2+}-mediated and Ca^{2+}-dependent currents, critical for oscillatory activity in thalamic neurons (Jahnsen and Llinas, 1984; Luthi and McCormick, 1998), are unnecessary in interneurons because interneuron MPOs persist in presence of Ca^{2+}-free extracellular solution or Ca^{2+} channel blocker Cd^{2+} (Chapman and Lacaille, 1999a). Thus, intrinsic MPOs in LM/RAD interneurons are produced by a cell-type specific interplay of voltage-gated Na^+ and K^+ currents, independent of I_h, I_M, voltage-gated Ca^{2+} currents, and Ca^{2+}-dependent K^+ currents (I_{KCa}).

Native somatodendritic A-type K^+ currents arise from multimeric K^+ channels composed of pore-forming α subunits of the Kv4 family (Sheng et al., 1992; Serodio et al., 1996; Song, 2002), in association with auxiliary subunits, like Kvβ subunits, K^+ channel interacting proteins, frequenin, and DPPX (for review, see Birnbaum et al., 2004). In CA1 hippocampus, a cell-type specific differential expression of Kv4 subtypes has been suggested with pyramidal cells highly expressing the Kv4.2 subtype and interneurons strongly expressing Kv4.3 (Martina et al., 1998; Serodio and Rudy, 1998; Lien et al. 2002; Rhodes et al., 2004). Moreover, A-type K^+ currents appeared predominantly mediated by Kv4.3 channels in CA1 stratum oriens/alveus interneurons (Lien

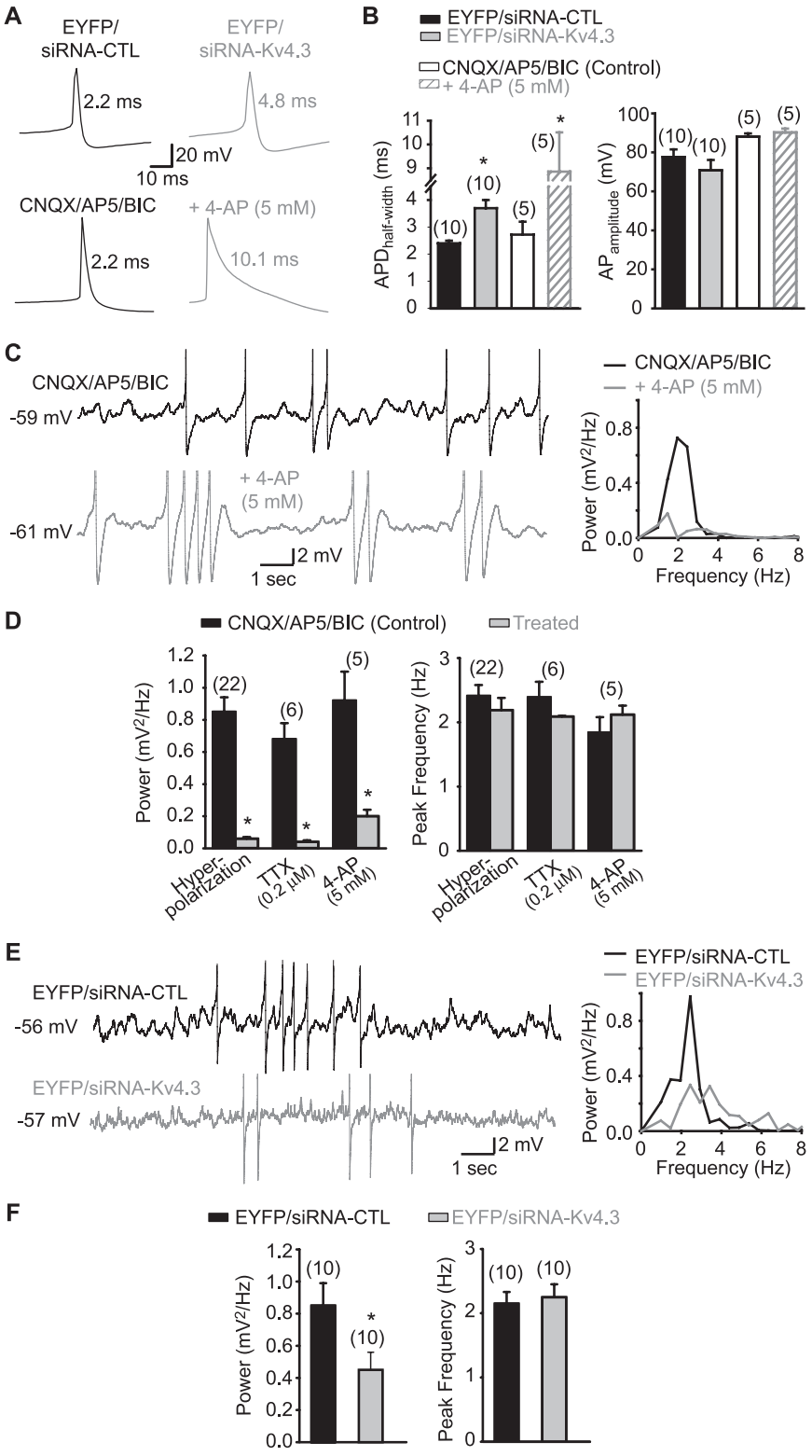

Figure 6. Kv4.3 siRNA broadens action potentials and inhibits MPOs in interneurons in slice cultures. ***A***, Representative traces of spontaneous action potentials in interneurons illustrating that Kv4.3 siRNA (top) and 4-AP (bottom) increase action potential duration. ***B***, Summary bar graphs indicating that $APD_{half\text{-}width}$ was significantly increased by either Kv4.3 siRNA compared with control siRNA or by 5 mM 4-AP (left), whereas action potential amplitude was unaffected by Kv4.3 siRNA or by 4-AP (right). ***C***, Representative traces (in presence of CNQX, AP5, and bicuculline) and corresponding power spectra for the same cell illustrating MPOs and the inhibitory effect of the K^+ channel blocker 4-AP (5 mM). ***D***, Summary bar graphs indicating that the power (left) but not the peak frequency (right) of MPOs is reduced by hyperpolarization, TTX, and 4-AP. ***E***, Representative traces and corresponding power spectra for the same cells showing that MPOs are decreased in interneurons transfected with Kv4.3 siRNA (bottom) compared with interneurons transfected with control siRNA (top). ***F***, Summary bar graphs demonstrating the significant reduction in MPO power (left) and unchanged peak frequency (right) by Kv4.3 siRNA compared with the control siRNA. $*p < 0.05$.

Table 1. Coexpression of Ca^{2+}-binding proteins and peptides with Kv4.3 in CA1 interneurons

	Number of cells in layer/total				Percentage coexpression with Kv4.3			
	O/A	PYR	RAD	LM	O/A	PYR	RAD	LM
Parvalbumin	3/84	81/84	0/84	0/84	0	12	0	0
Calbindin	5/31	10/31	6/31	10/31	20	20	50	70
Somatostatin	52/58	5/58	1/58	0/58	13	80	0	0
Cholecystokinin	5/28	4/28	3/28	16/28	0	25	33	88

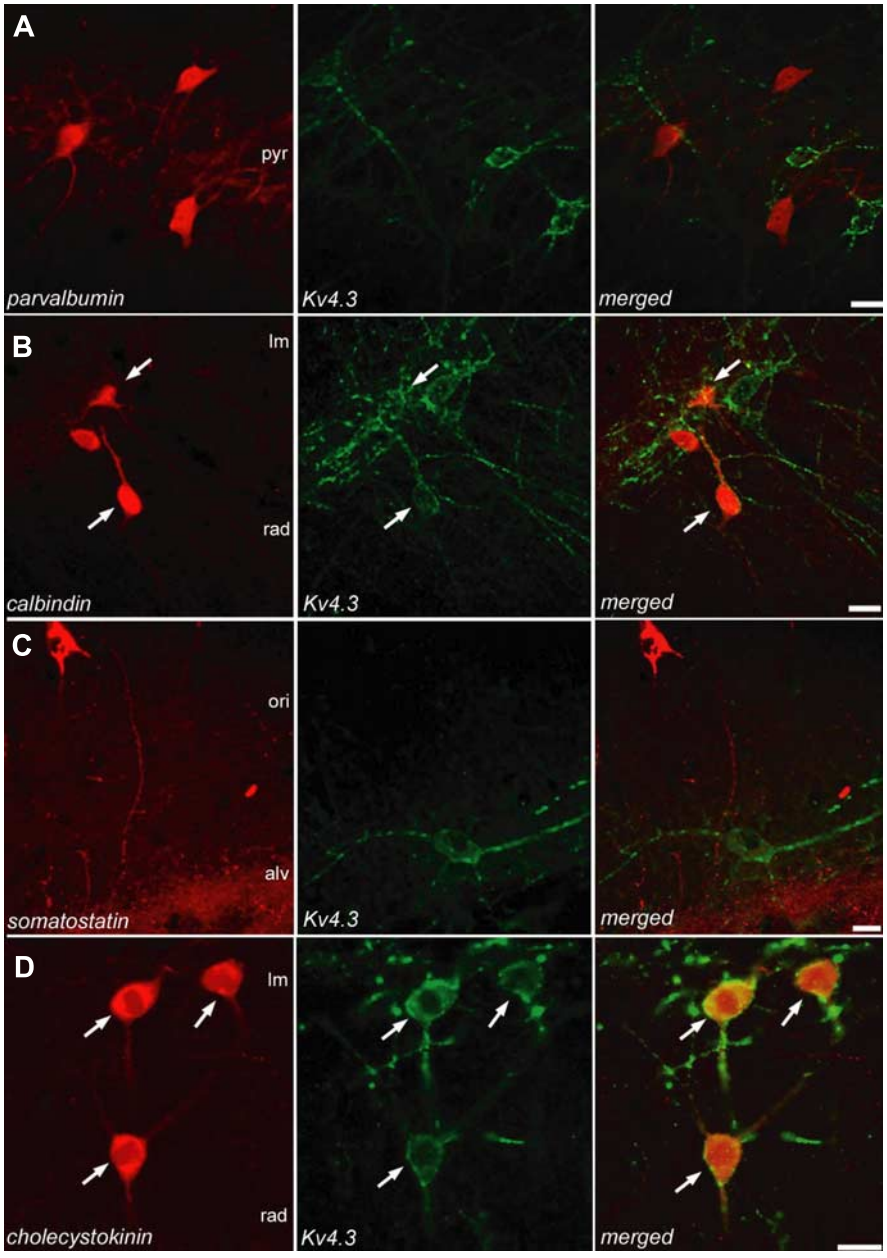

Figure 7. Specific subpopulations of CA1 interneurons coexpressing Kv4.3 and Ca^{2+}-binding proteins or peptides. ***A***, Confocal image of parvalbumin-immunopositive interneurons located in stratum pyramidale (left). Confocal image of immunolabeling for Kv4.3 in the same section (middle) and the merged images (right) indicate that parvalbumin-positive interneurons mostly did not colocalize Kv4.3. ***B***, Calbindin-positive neurons (left) in stratum radiatum and lacunosum-moleculare often colocalized Kv4.3 (middle, right). Arrows point to double-labeled interneurons. ***C***, Somatostatin-positive interneurons (left) in stratum oriens (ori) and alveus (alv) mostly did not colocalize Kv4.3 (middle, right). ***D***, Cholecystokinin-immunopositive interneurons in stratum radiatum and lacunosum-moleculare (left) highly colocalized Kv4.3 (middle, right). Scale bars, 15 μm.

et al., 2002). We obtained multiple lines of evidence indicating that Kv4.3 mediates A-type K^+ currents in LM/RAD interneurons. First, LM/RAD interneurons with A-type K^+ currents in voltage-clamp recordings were identified as Kv4.3 immunopositive, indicating that A-type K^+ current presence was correlated with Kv4.3 expression in the same cell. Second, Kv4.3 expression in HEK293 cells was sufficient to generate A-type K^+ currents. Third, transfection of a siRNA sequence targeting Kv4.3 mRNA selectively inhibited Kv4.3-mediated A-type K^+ currents in HEK293 cells, as well as native A-type K^+ currents in LM/RAD interneurons in slice cultures. This K^+ current functional knockdown was unlikely a nonspecific effect of siRNA transfection because A-type K^+ currents were selectively diminished, and delayed rectifier K^+ currents, mediated by Kv subunits other than Kv4 (Coetzee et al., 1999; Song, 2002), were unchanged in interneurons. Additionally, Kv4.3 siRNA effects were cell-type specific because CA1 pyramidal cell A-type K^+ currents, thought to be mediated by Kv4.2 (Serodio and Rudy, 1998; Rhodes et al., 2004; Kim et al., 2005), were unaltered.

Having identified Kv4.3 as a K^+-channel subunit mediating LM/RAD interneuron A-type K^+ currents enabled us to show directly that A-type K^+ currents contribute to MPOs in these cells. Using Kv4.3 siRNA transfection of LM/RAD interneurons in slice cultures, we uncovered clear impairment of MPOs after A-type K^+ current functional knockdown. These results were entirely consistent with our findings of clear correlation between Kv4.3 expression and MPOs in individual interneurons with current-clamp recordings and Kv4.3 immunodetection. Moreover, compatible with known roles of A-type K^+ currents in regulating action potential onset and shape (Rudy, 1988; Zhang and McBain, 1995b; Hoffman et al., 1997; Kim et al., 2005), Kv4.3 siRNA transfection resulted in a significant broadening of interneuron action potentials (see also Shibata et al., 2000; Yuan et al., 2005). Overall, our results clearly show that A-type K^+ current functional knockdown by Kv4.3 siRNA significantly impaired LM/RAD interneuron MPOs, revealing an essential role for Kv4.3-mediated A-type currents in generating such intrinsic rhythmic activity in hippocampal interneurons. Our results are consistent with pharmacological evidence that interneuron A-type K^+ currents (Lien et al. 2002) and MPOs (Chapman and Lacaille 1999a) are sensitive to the K^+

channel blocker 4-AP but not to TEA. However, our results do not rule out that other K^+ currents sensitive to 4-AP and Ba^{2+} (Chapman and Lacaille 1999a) might also contribute to MPOs. Indeed, our observation that 4-AP effects on MPOs are larger than Kv4.3 siRNA effects suggests that other 4-AP sensitive K^+ currents may also contribute. It is unlikely that fast delayed rectifier K^+ currents are necessary because they are blocked by TEA (Lien et al. 2002), whereas MPOs are not affected (Chapman and Lacaille 1999a). However, certain Kv1 channels that underlie dendrotoxin-sensitive K^+ currents (I_D) and that operate at subthreshold membrane potentials are resistant to TEA but sensitive to 4-AP (Coetzee et al. 1999) and Ba^{2+} (Hurst et al. 1995). Although dendrotoxin-sensitive I_D currents were reportedly absent in CA1 oriens/alveus interneurons (Zhang and McBain, 1995a; Lien et al. 2002), they could be present in specific interneuron subtypes like LM/RAD cells. Additional work will be important to resolve a possible additional contribution of I_D currents to MPOs in LM/RAD interneurons.

Our recordings of prominent A-type K^+ currents in outside-out patches from LM/RAD interneurons are also consistent with a cell-specific role of A-type K^+ currents in MPOs. Although interneurons in stratum oriens/alveus exhibit A-type currents (Zhang and McBain, 1995b), specific interneuron cell types in LM/RAD were reported previously to display much more prominent A-type currents in dissociated cells from CA1 area (Fan and Wong, 1996). Our results with LM/RAD interneurons in acutely isolated slices demonstrate that A-type K^+ currents in outside-out patches exhibit a window of activation corresponding to the subthreshold membrane potentials at which MPOs are observed, suggesting that A-type K^+ current gating properties are compatible with a role in MPO generation in these interneurons. Moreover, using double immunofluorescence against Kv4.3 and interneuron-specific cell markers like Ca^{2+}-binding proteins and peptides, we uncovered distinct interneuron subpopulations preferentially expressing Kv4.3 subunits. Although Kv4.3-immunopositive interneurons were found in all hippocampal layers (Rhodes et al., 2004), they colabeled with cholecystokinin-positive interneurons of LM, calbindin-positive interneurons of RAD and LM, and somatostatin-positive interneurons of PYR. Thus, Kv4.3 may be important for A-type K^+ currents and regulation of somatodendritic excitability in these specific interneuron subpopulations, supporting an interneuron subtype-specific role of Kv4.3 in MPOs and, consequently, in hippocampal rhythmic activity.

Hippocampal theta rhythmic activity *in vivo* is driven by a combination of extrinsic inputs and network interactions between pyramidal cells and inhibitory interneurons (Buzsaki, 2002; Klausberger et al., 2003; Somogyi and Klausberger, 2005). Our work further indicates that such rhythmic activity likely involves additional synergistic interactions with intrinsic membrane conductances of individual interneurons, as suggested for CA1 pyramidal cells (Konopacki et al., 1987; MacVicar and Tse, 1989; Leung and Yim, 1991; Chapman and Lacaille, 1999b) and entorhinal stellate cells (Klink and Alonso, 1993). Thus, our findings identify a critical contribution of Kv4.3-mediated A-type K^+ currents in MPOs in specific interneuron subpopulations that may be important for hippocampal rhythmic theta activity. Such a role in regulation of rhythmic activity expands the function of neuronal A-type K^+ currents beyond their previously established roles in regulation of firing rate (Rudy, 1988), action potential waveform (Zhang and McBain, 1995b), and dendritic signaling (Hoffman et al., 1997).

References

Alonso A, Llinas RR (1989) Subthreshold Na^+-dependent theta-like rhythmicity in stellate cells of entorhinal cortex layer II. Nature 342:175–177.

Alonso A, Llinas RR (1992) Electrophysiology of the mammillary complex in vitro. II. Medial mammillary neurons. J Neurophysiol 68:1321–1331.

Barry DM, Xu H, Schuessler RB, Nerbonne JM (1998) Functional knockout of the transient outward current, long-QT syndrome, and cardiac remodeling in mice expressing a dominant-negative Kv4 alpha subunit. Circ Res 83:560–567.

Birnbaum SG, Varga AW, Yuan LL, Anderson AE, Sweatt JD, Schrader LA (2004) Structure and function of Kv4-family transient potassium channels. Physiol Rev 84:803–833.

Bland BH (1986) The physiology and pharmacology of hippocampal formation theta rhythms. Prog Neurobiol 26:1–54.

Buzsaki G (2002) Theta oscillations in the hippocampus. Neuron 33:325–340.

Cantero JL, Atienza M, Stickgold R, Kahana MJ, Madsen JR, Kocsis B (2003) Sleep-dependent theta oscillations in the human hippocampus and neocortex. J Neurosci 23:10897–10903.

Chapman CA, Lacaille JC (1999a) Intrinsic theta-frequency membrane potential oscillations in hippocampal CA1 interneurons of stratum lacunosum-moleculare. J Neurophysiol 81:1296–1307.

Chapman CA, Lacaille JC (1999b) Cholinergic induction of theta-frequency oscillations in hippocampal inhibitory interneurons and pacing of pyramidal cell firing. J Neurosci 19:8637–8645.

Coetzee WA, Amarillo Y, Chiu J, Chow A, Lau D, McCormack T, Moreno H, Nadal MS, Ozaita A, Pountney D, Saganich M, Vega-Saenz de Miera E, Rudy B (1999) Molecular diversity of K^+ channels. Ann NY Acad Sci 868:233–285.

Cotella D, Jost N, Darna M, Radicke S, Ravens U, Wettwer E (2005) Silencing the cardiac potassium channel Kv4.3 by RNA interference in a CHO expression system. Biochem Biophys Res Commun 330:555–560.

Dickson CT, Magistretti J, Shalinsky MH, Fransen E, Hasselmo ME, Alonso A (2000) Properties and role of I(h) in the pacing of subthreshold oscillations in entorhinal cortex layer II neurons. J Neurophysiol 83:2562–2579.

Fan SH, Wong RK (1996) Selective expression of transient outward currents in different types of acutely isolated hippocampal interneurons. J Neurophysiol 76:3563–3567.

Fischer Y, Gahwiler BH, Thompson SM (1999) Activation of intrinsic hippocampal theta oscillations by acetylcholine in rat septo-hippocampal cocultures. J Physiol (Lond) 519:405–413.

Freund TF, Buzsaki G (1996) Interneurons of the hippocampus. Hippocampus 6:347–470.

Govek EE, Newey SE, Akerman CJ, Cross JR, Van der Veken L, Van Aelst L (2004) The X-linked mental retardation protein oligophrenin-1 is required for dendritic spine morphogenesis. Nat Neurosci 7:364–372.

Hoffman DA, Magee JC, Colbert CM, Johnston D (1997) K^+ channel regulation of signal propagation in dendrites of hippocampal pyramidal neurons. Nature 387:869–875.

Hu H, Vervaeke K, Storm JF (2002) Two forms of electrical resonance at theta frequencies, generated by M-current, h-current and persistent Na^+ current in rat hippocampal pyramidal cells. J Physiol (Lond) 545:783–805.

Hurst RS, Latorre R, Toro L, Stefani E (1995) External barium block of Shaker potassium channels: evidence for two binding sites. J Gen Physiol 106:1069–1087.

Jahnsen H, Llinas R (1984) Ionic basis for the electro-responsiveness and oscillatory properties of guinea-pig thalamic neurones *in vitro.* J Physiol (Lond) 349:227–247.

Kim J, Wei DS, Hoffman DA (2005) Kv4 potassium channel subunits control action potential repolarization and frequency-dependent broadening in rat hippocampal CA1 pyramidal neurones. J Physiol (Lond) 569:41–57.

Klausberger T, Magill PJ, Marton LF, Roberts JD, Cobden PM, Buzsaki G, Somogyi P (2003) Brain-state- and cell-type-specific firing of hippocampal interneurons *in vivo.* Nature 421:844–848.

Klink R, Alonso A (1993) Ionic mechanisms for the subthreshold oscillations and differential electroresponsiveness of medial entorhinal cortex layer II neurons. J Neurophysiol 70:144–157.

Kollo M, Holderith NB, Nusser Z (2006) Novel subcellular distribution pattern of A-type K^+ channels on neuronal surface. J Neurosci 26:2684–2691.

Konopacki J, MacIver MB, Bland BH, Roth SH (1987) Carbachol-induced EEG "theta" activity in hippocampal brain slices. Brain Res 405:196–198.

Leung LW, Yim CY (1991) Intrinsic membrane potential oscillations in hippocampal neurons *in vitro*. Brain Res 553:261–274.

Lien CC, Martina M, Schultz JH, Ehmke H, Jonas P (2002) Gating, modulation and subunit composition of voltage-gated K(+) channels in dendritic inhibitory interneurones of rat hippocampus. J Physiol (Lond) 538:405–419.

Locke RE, Nerbonne JM (1997) Three kinetically distinct Ca^{2+}-independent depolarization-activated K^+ currents in callosal-projecting rat visual cortical neurons. J Neurophysiol 78:2309–2320.

Luthi A, McCormick DA (1998) Periodicity of thalamic synchronized oscillations: the role of Ca^{2+}-mediated upregulation of I_h. Neuron 20:553–563.

Maccaferri G, McBain CJ (1996) The hyperpolarization-activated current (I_h) and its contribution to pacemaker activity in rat CA1 hippocampal stratum oriens-alveus interneurones. J Physiol (Lond) 497:119–130.

MacVicar BA, Tse FW (1989) Local neuronal circuitry underlying cholinergic rhythmical slow activity in CA3 area of rat hippocampal slices. J Physiol (Lond) 417:197–212.

Martina M, Schultz JH, Ehmke H, Monyer H, Jonas P (1998) Functional and molecular differences between voltage-gated K^+ channels of fast-spiking interneurons and pyramidal neurons of rat hippocampus. J Neurosci 18:8111–8125.

Mitchell SJ, Rawlins JN, Steward O, Olton DS (1982) Medial septal area lesions disrupt theta rhythm and cholinergic staining in medial entorhinal cortex and produce impaired radial arm maze behavior in rats. J Neurosci 2:292–302.

Nunez A, Garcia-Austt E, Buno Jr W (1987) Intracellular theta-rhythm generation in identified hippocampal pyramids. Brain Res 416:289–300.

Petsche H, Stumpf C, Gogolak G (1962) The significance of the rabbit's septum as a relay station between the midbrain and the hippocampus. I. The control of hippocampus arousal activity by the septum cells. Electroencephalogr Clin Neurophysiol 14:202–211.

Rhodes KJ, Carroll KI, Sung MA, Doliveira LC, Monaghan MM, Burke SL, Strassle BW, Buchwalder L, Menegola M, Cao J, An WF, Trimmer JS (2004) KChIPs and Kv4 alpha subunits as integral components of A-type potassium channels in mammalian brain. J Neurosci 24:7903–7915.

Rudy B (1988) Diversity and ubiquity of K channels. Neuroscience 25:729–749.

Serodio P, Rudy B (1998) Differential expression of Kv4 K^+ channel subunits mediating subthreshold transient K^+ (A-type) currents in rat brain. J Neurophysiol 79:1081–1091.

Serodio P, Vega-Saenz de Miera E, Rudy B (1996) Cloning of a novel component of A-type K^+ channels operating at subthreshold potentials with unique expression in heart and brain. J Neurophysiol 75:2174–2179.

Sheng M, Tsaur ML, Jan YN, Jan LY (1992) Subcellular segregation of two A-type K^+ channel proteins in rat central neurons. Neuron 9:271–284.

Shi H, Wang HZ, Wang Z (2000) Extracellular Ba^{2+} blocks the cardiac transient outward K^+ current. Am J Physiol Heart Circ Physiol 278:H295–H299.

Shibata R, Nakahira K, Shibasaki K, Wakazono Y, Imoto K, Ikenaka K (2000) A-type K^+ current mediated by the Kv4 channel regulates the generation of action potential in developing cerebellar granule cells. J Neurosci 20:4145–4155.

Somogyi P, Klausberger T (2005) Defined types of cortical interneurone structure space and spike timing in the hippocampus. J Physiol (Lond) 562:9–26.

Song WJ (2002) Genes responsible for native depolarization-activated K^+ currents in neurons. Neurosci Res 42:7–14.

Song WJ, Tkatch T, Baranauskas G, Ichinohe N, Kitai ST, Surmeier DJ (1998) Somatodendritic depolarization-activated potassium currents in rat neostriatal cholinergic interneurons are predominantly of the A type and attributable to coexpression of Kv4.2 and Kv4.1 subunits. J Neurosci 18:3124–3137.

Stoppini L, Buchs PA, Muller D (1991) A simple method for organotypic cultures of nervous tissue. J Neurosci Methods 37:173–182.

Vinogradova OS (1995) Expression, control, and probable functional significance of the neuronal theta-rhythm. Prog Neurobiol 45:523–583.

Winson J (1978) Loss of hippocampal theta rhythm results in spatial memory deficit in the rat. Science 201:160–163.

Yu SP, Kerchner GA (1998) Endogenous voltage-gated potassium channels in human embryonic kidney (HEK293) cells. J Neurosci Res 52:612–617.

Yuan W, Burkhalter A, Nerbonne JM (2005) Functional role of the fast transient outward K^+ current I_A in pyramidal neurons in (rat) primary visual cortex. J Neurosci 25:9185–9194.

Zhang L, McBain CJ (1995a) Voltage-gated potassium currents in stratum oriens-alveus inhibitory neurones of the rat CA1 hippocampus. J Physiol (Lond) 488:647–660.

Zhang L, McBain CJ (1995b) Potassium conductances underlying repolarization and after-hyperpolarization in rat CA1 hippocampal interneurones. J Physiol (Lond) 488:661–672.